



Full length article

Crustal deformation of the southeastern corner of Egypt derived from geodetic data

Mohamed Saleh^a, Kamal Sakr^a, Mohamed Rashwan^{a,*}, Karrar El-Faragawy^b, Mohamed El-Dabaa^a^a National Research Institute of Astronomy and Geophysics, Helwan, Egypt^b Geology Department, Faculty of Science, Aswan University, Aswan, Egypt

ARTICLE INFO

Keywords:

Crustal movements
GPS
Abu-Dabbab
Lake Nasser
Egypt

ABSTRACT

The proper evaluation of the crustal deformation is important prior to any strategic projects. Due to the importance of the southeastern corner of Egypt which contains many mineral resources beside a lot of attractive tourism places, we have selected this area to estimate the recent crustal movements and its relation to earthquake activities within this region using the available GPS and seismicity measurements. We used 19 permanent and campaign GPS sites in and around the study area that cover the time span 2007–2014. Most of these sites are related to Abu-Dabbab and Lake Nasser networks. The obtained GPS results show that there is an observed deformation in Abu-Dabbab area, along Red Sea coast, which characterized by a seismic cluster. The localization of the observed movements at Abu-Dabbab area may indicate that the deformation is related to a local structure within the study area. On the other hand, GPS sites located East of Lake Nasser and the permanent GPS sites in southern Egypt do not show any significant velocity field and it seems to be stable compared to Abu-Dabbab region. Even with the non-uniform spatial resolution of the GPS sites used in this work, our results are in good agreement with the seismicity of the study area.

1. Introduction

The Eastern border of the study area, southeastern part of Egypt, is the Red Sea; starting from Safaga to Shalaten in the South, and the Western border is the Nile River. The area is considered as one of the most promising areas in Egypt, because it is an attractive environment for tourism in addition to many natural resources such as Phosphates, Silica, Feldspars, and Gold mines. As shown in the seismicity of Egypt in Fig. 1, Egypt is generally characterized by low-moderate earthquake activity. Most of the recorded events in Egypt are less than 3 M_L . The distribution of seismic events in Egypt shows some areas of seismic clusters. The study area includes regions with seismic clusters such as Abu-Dabbab, Shalaten, Idfu and Aswan clusters. Abu-Dabbab and Aswan are the most active regions in this area and a ground deformation is expected within these regions. The biggest earthquake occurred in Aswan area was the November 11, 1981 with a magnitude of 5.6 M_L located 60 km Southwest of Aswan High dam. It is also called Kalabsha earthquake, since the epicenter was located close to Kalabsha fault west of the Lake. Most of seismic activities around Lake Nasser is concentrated along the intersection between active East-West Kalabsha and Sayal faults with the North-South Kurkur and Khor El-Ramal faults,

West of the Lake (Hussein et al., 2013; Telesca et al., 2017).

East of the Lake there is no significant seismic activity recorded. The selected study area in this work is covered only the area East of the Lake. Therefore, the most active region in our study area is Abu-Dabbab area. The November 12, 1955 and July 2, 1984 are the most significant earthquakes recorded in Abu-Dabbab area with magnitudes of 6.1 M_b and 5.1 M_b , respectively. Recent seismic records shows that Abu Dabbab area is one of the most active tectonic zones along the Red Sea (Badawy et al., 2008; Hussein et al., 2011). Generally, The tectonic setting of this region is mainly controlled by the Red Sea opening (Martinez and Cochran, 1988). Many fault zones perpendicular to the Red Sea coastline are generated due to the this opening process. The seismicity of Abu-Dabbab area shows a seismic cluster that extends offshore in the Red Sea with a direction NEE-SWW, approximately perpendicular to the Red Sea coast, which may be related to one of the these transform fault (El Khrepy et al., 2015).

Most of the study area is located within the Arabian–Nubian shield, the eastern part of Egypt. Due to the effect of strong erosion, the basement appears on the ground and most of the Phanerozoic sediments are eroded. As shown in Fig. 2, two major tectonostratigraphic units are exist, Lower infrastructure unites where comprise high to medium

Peer review under responsibility of National Research Institute of Astronomy and Geophysics.

* Corresponding author.

E-mail address: m2000_rashwan@yahoo.com (M. Rashwan).<https://doi.org/10.1016/j.nrjag.2018.05.005>

Received 13 February 2018; Received in revised form 4 April 2018; Accepted 19 May 2018

Available online 24 May 2018

2090-9977/ © 2018 Published by Elsevier B.V. on behalf of National Research Institute of Astronomy and Geophysics This is an open access article under the CC BY-NC-ND license (<http://creativecommons.org/licenses/by-nc-nd/4.0/>).

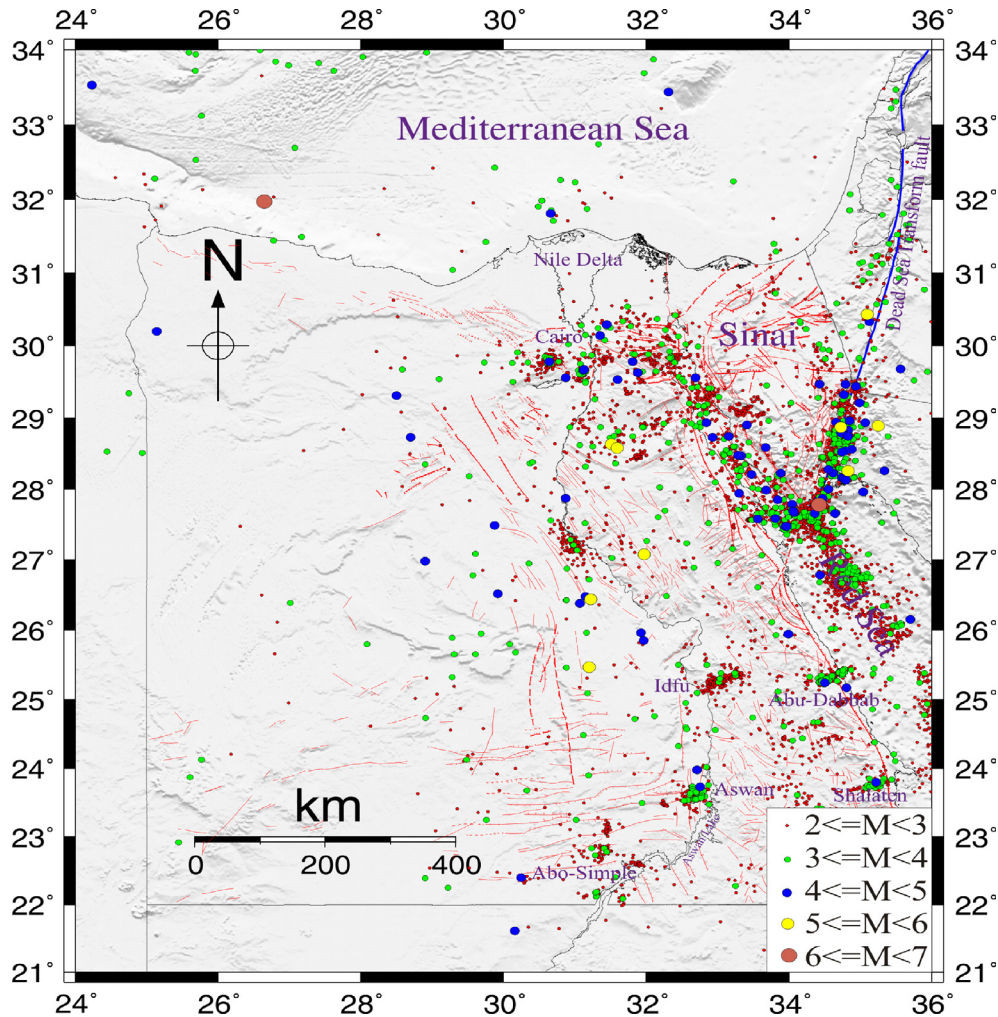


Fig. 1. Seismicity of Egypt during the period from 1997 to 2014 based on the data of ENSN. Red lines are the surface faults in Egypt (Egyptian Geological Survey and Mining Authority, EGSM, 1981). Blue line is the Dead Sea Fault. (For interpretation of the references to colour in this figure legend, the reader is referred to the web version of this article.)

grade metamorphic Gneisses and upper infrastructure units where include low grade, arc/back arc volcano-sedimentary associations with slabs of dismembered Ophiolites; commonly known as Pan-African Nappe complex, (Gass, 1982, Kröner et al., 1992; Neumayr et al., 1998).

In this paper we are trying to estimate the recent crustal movements of this area by using the available GPS data and try to link it with the recorded seismic activities. The available data, the processing strategies, and error assessment will be presented in Section 2. Section 3 contains the achieved results, and finally the discussion and conclusion will be presented in Section 4.

2. Data Processing

We used all the archived GPS data recorded within the study area between 2007 and 2014. As shown in Fig. 3, most of the GPS sites in the study area are related to the campaign Ab-Dabbab and Lake Nasser networks. Abu-Dabbab network was established in October 2008 and in this work we have used all the archived data from this network. Lake Nasser network is one of the oldest campaign GPS networks in Egypt. From this network, just four sites were used (MNAM, DAHM, BEER, and ALAK). Seven campaigns from Abu-Dabbab network and nine campaigns from Lake Nasser network are used in this work. Beside the

campaign data we used all the permanent sites in Egypt from the Egyptian Permanent GPS Network (EPGN) which available in the measurement days of the campaign sites. Fig. 4 shows the available data from both permanent and campaign sites.

We added to the Egyptian sites, permanent and campaign, a data of 34 permanent stations from IGS (International GNSS Service) and SOPAC (Scripps Orbit and Permanent Array Center) (see Fig. 5). The aim from using these stations is to set a good configuration around the Egyptian stations. Moreover, we used 29 sites out of these 34 for the datum definition, since they are included in the International Terrestrial Reference Frame 2008 (ITRF2008, (Altamimi et al., 2011)).

GPS data were processed using Bernese GPS Software Ver. 5.0 (Dach et al., 2007), which resulted in a 87 daily solutions in ITRF2008 reference frame. The processing was carried out using the following constraints:

1. ITRF2008 reference frame,
2. NNR-NUVEL-1A plate motion model for non-ITRF stations,
3. Usage the reprocessed CODE products till end 2010 and the final IGS products for the remaining period, 2011–2014,
4. Automatic baseline creation using MAX-OBS strategy,
5. Ionosphere free linear combination L_{IF} ,

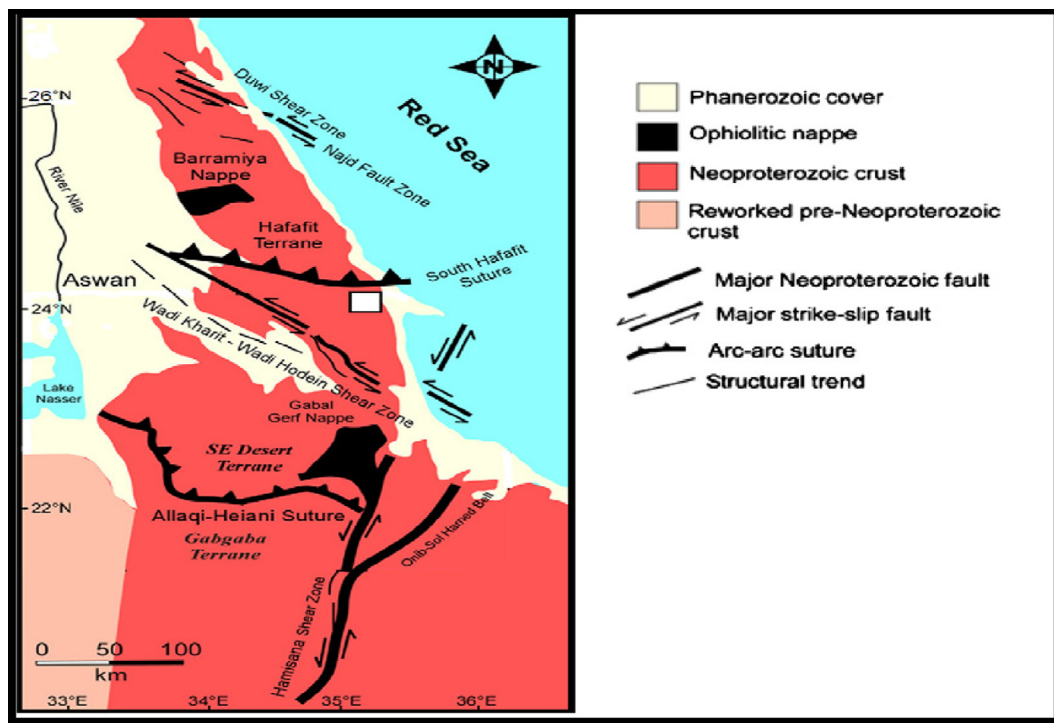


Fig. 2. Simplified geological and tectonic maps of the Southeastern corner of Egypt (modified after [Abdeen and Abdelghaffar, 2011](#)).

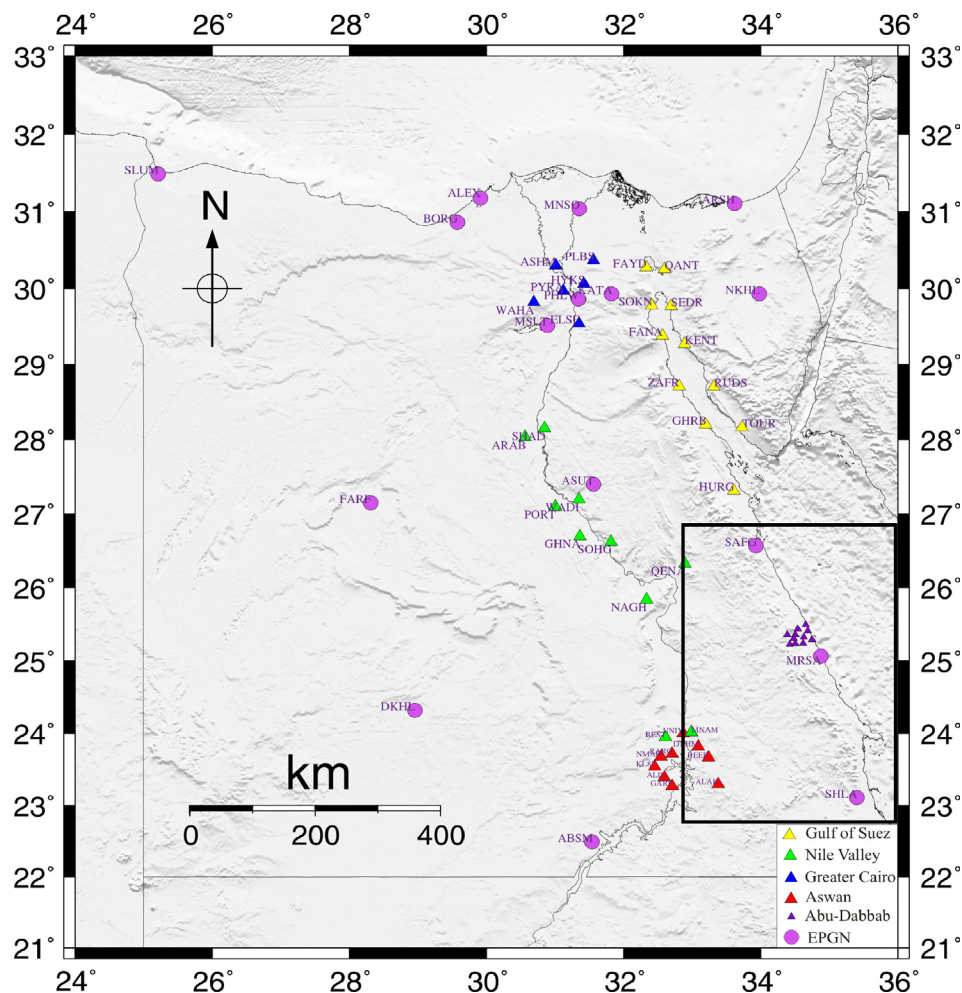


Fig. 3. Geographic distribution of the Egyptian GPS stations. Black box is the study area.

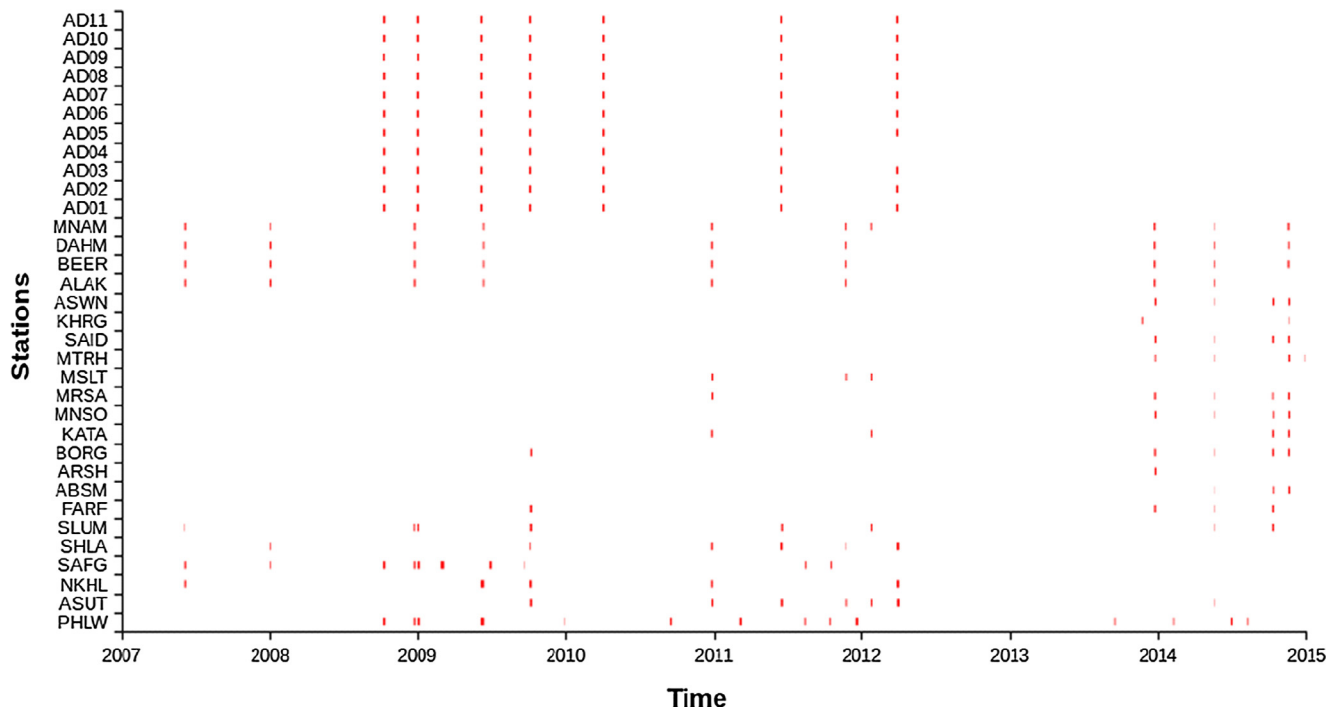


Fig. 4. Availability of the EPGN stations and the campaign data for the period 2007–2014.

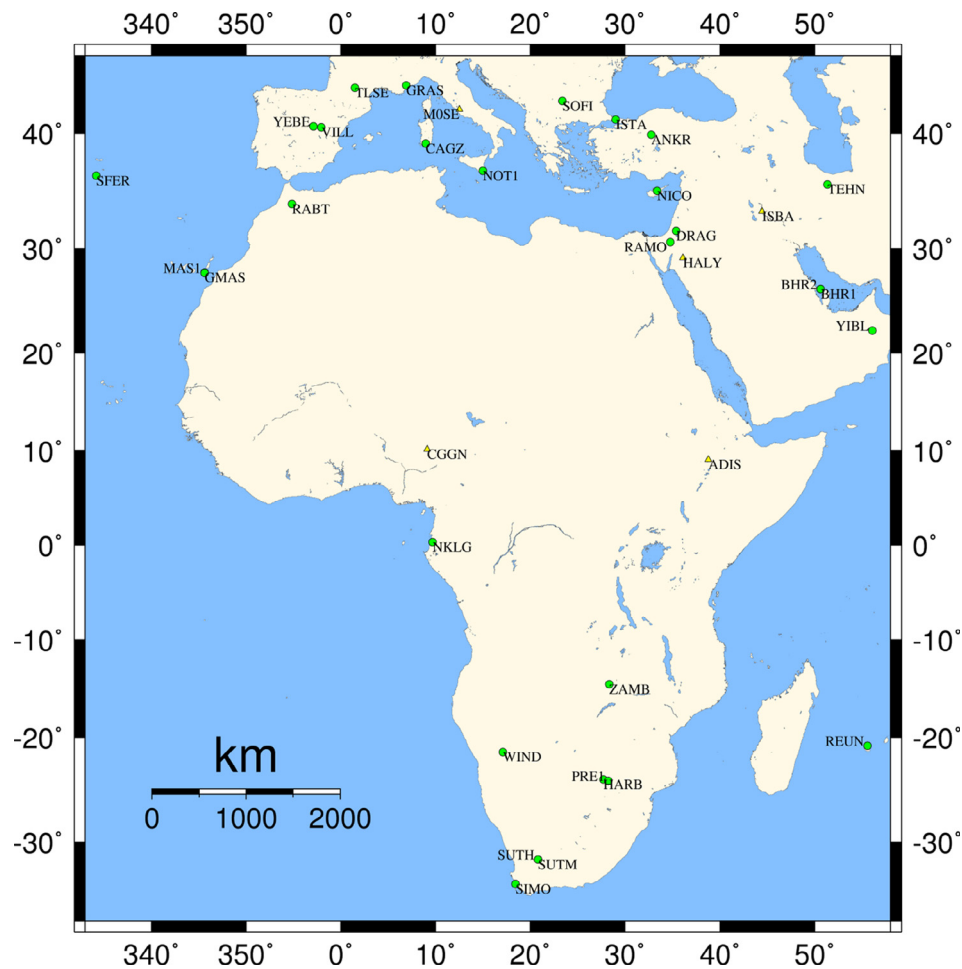


Fig. 5. Selected IGS permanent Stations that used during the processing. Green dots represent stations used for datum definition. (For interpretation of the references to colour in this figure legend, the reader is referred to the web version of this article.)

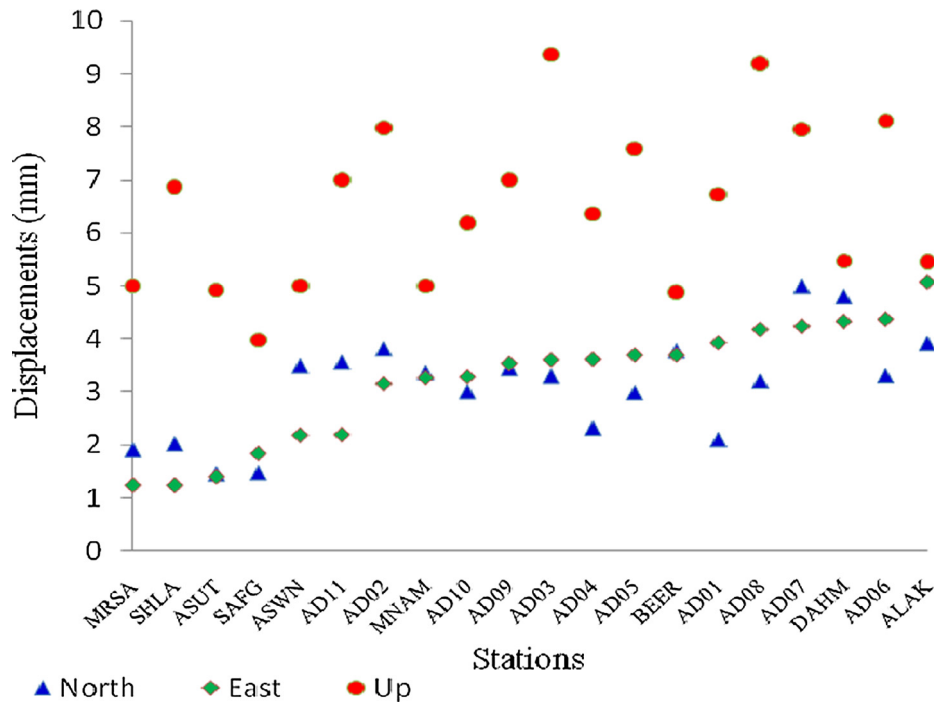


Fig. 6. Repeatability of stations within study area (permanent and campaign sites).

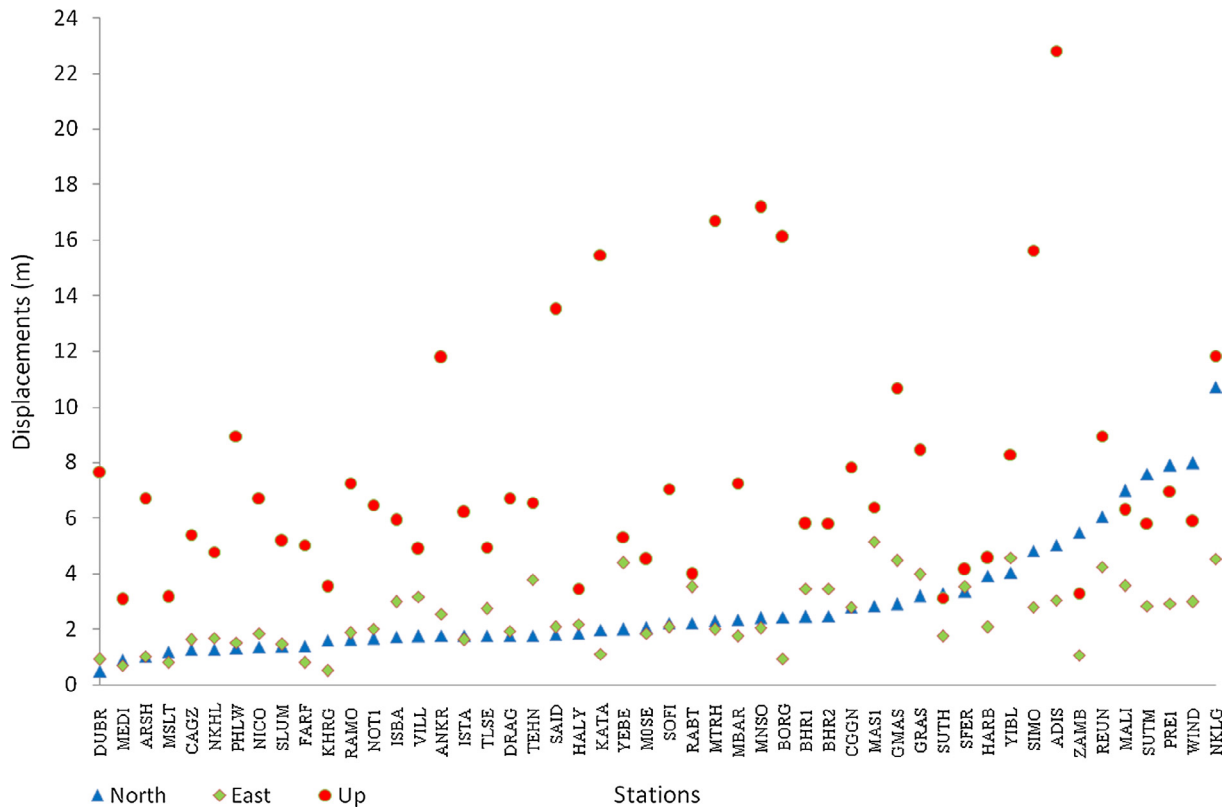


Fig. 7. Repeatability of Selected IGS and SOPAC permanent stations.

- 6. Elevation cut-off angle 3°, and
- 7. Dry Niell as troposphere model with GMF (Global Mapping function) as mapping function.

Afterward, we combined all the daily solutions to get one solution (coordinates and velocities) in ITRF08 datum by using the 29 permanent sites. One important product resulted from the combination

Table 1
Station position in terms of Longitude and Latitude, absolute horizontal velocities in ITRF-08, velocities in Nubia-fixed reference frame and the scaled error generated by the scaling of the co-variance matrix.

Station	Location		ITRF-08 velocities mm/yr		Nubia-fixed velocities mm/yr		Scaled standard (σ_s) mm	
	Lon.	Lat.	East	North	East	North	East	North
AD01	34.66	25.50	22.60	23.10	3.21	3.02	1.96	1.40
AD02	34.54	25.44	19.90	20.20	0.51	0.12	1.57	2.55
AD03	34.50	25.36	18.50	19.30	−0.90	−0.80	1.80	2.20
AD04	34.38	25.36	17.90	19.20	−1.50	−0.90	1.80	1.16
AD05	34.42	25.23	21.00	20.60	1.61	0.52	1.84	1.99
AD06	34.50	25.24	17.90	20.90	−1.5	0.82	2.18	2.21
AD07	34.62	25.24	19.30	19.10	−0.95	−0.99	2.11	3.33
AD08	34.75	25.29	20.40	19.50	1.01	−0.59	2.08	2.14
AD09	34.69	25.41	19.60	18.70	0.21	−1.39	1.76	2.30
AD10	34.63	25.33	18.40	18.10	−1.00	−1.99	1.64	2.01
AD11	34.48	25.31	19.70	18.70	0.31	−1.39	1.09	2.38
ALAK	33.38	23.29	19.30	20.10	−0.10	0.02	2.53	2.61
BEER	33.24	23.66	18.80	20.10	−0.60	0.02	1.84	2.52
DAHM	33.09	23.82	20.10	20.60	0.71	0.52	2.16	3.20
MNAM	32.99	24.02	20.00	19.60	0.61	−0.49	1.63	2.24
MRSA	34.88	25.07	19.80	21.00	0.41	0.92	0.62	0.95
ASWN	32.85	23.97	19.60	19.00	0.11	0.42	0.72	1.16
SAFG	33.93	26.57	19.50	20.50	−3.2	3.52	0.92	0.98
SHLA	35.40	23.11	16.20	23.60	3.21	3.02	1.86	2.52

process is the stations repeatability for each component (North, East, and Up). The repeatability is the residuals of the daily solutions with respect to the combined solution, which reflects somehow the accuracy of our solution. As it known that the standard deviations estimated from Bernese is too optimistic due to the absence of the time correlation, we used the repeatability values to scale the co-variance matrix and obtain more realistic error assessment (Saleh and Becker, 2014). Fig. 6 shows the repeatability of the GPS stations within the study area. The repeatability in the horizontal component is 1–2 mm for permanent stations and 2–4 mm for the campaign sites. The values are much higher in the Up component, which reach up to 9 mm. The situation is a bit similar in case of IGS and SOPAC sites, as shown in Fig. 7, 1–4 mm in the horizontal component and up to 9 mm in the Up component with a clear appearance of some outliers especially in the Up component. As shown in Table 1, The obtained results of scaled error show more realistic values, which ranging from 0.7 to 3.0 mm in the horizontal component and 2.4–5.1 mm in the vertical component.

3. Results

Fig. 8 shows the achieved horizontal velocity in ITRF08 for all the processed stations. It is clear that all sites are moving toward the Northeast direction with a magnitude close to 30 mm/yr. Focusing on the study area, as shown in Fig. 9, that all of the Egyptian stations within the study area are moving toward the Northeast direction with

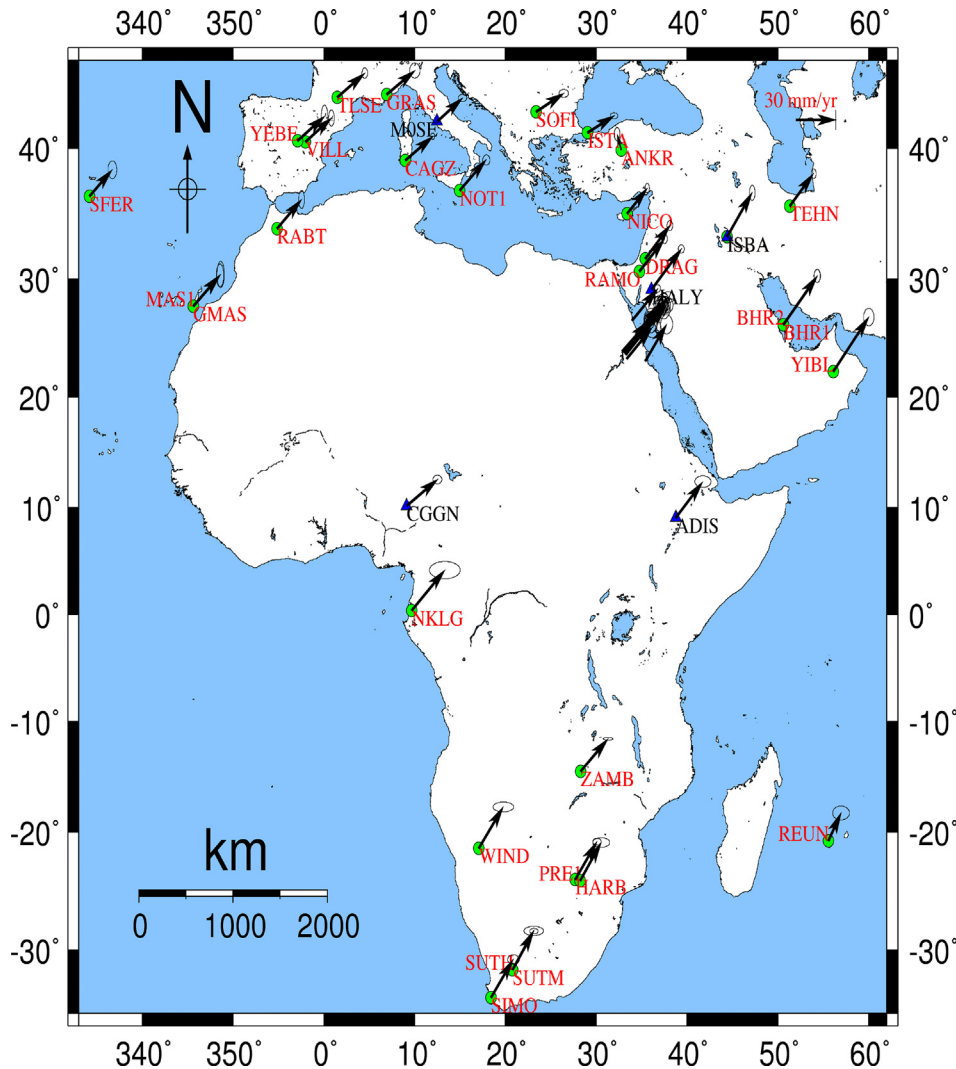


Fig. 8. ITRF-08 horizontal velocities for all the processed station, permanent and epoch, with 95% confidence region.

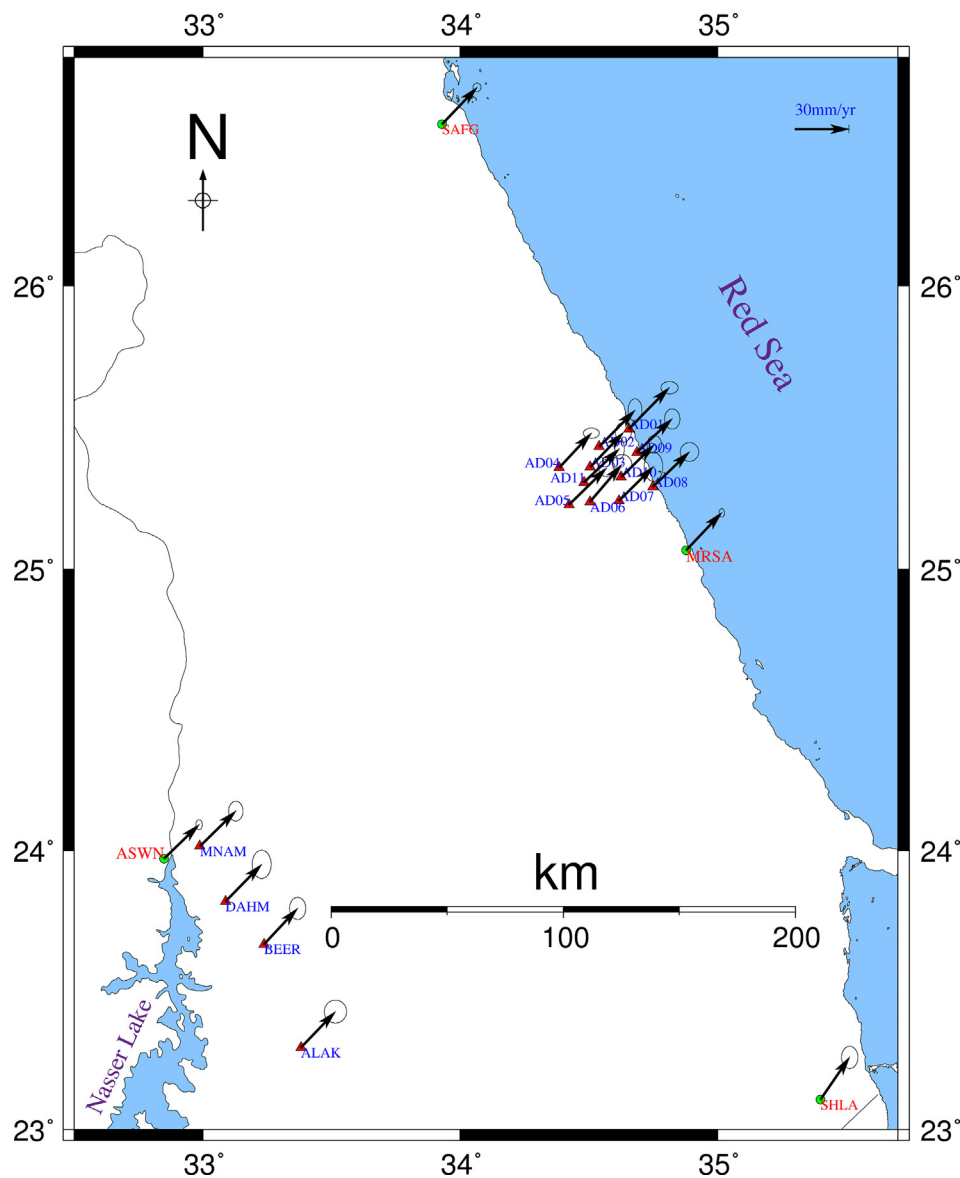


Fig. 9. Focus on the study area, ITRF-08 absolute horizontal velocities with 95% confidence region.

an average magnitude of 28 mm/yr which is similar to rates previously estimated by (Saleh and Becker, 2014) who estimated an average magnitude of absolute velocity field in ITRF08 for all Egyptian stations of 28–30 mm/yr. Within the study area, all sites indicate a significant horizontal movements with 95% of the confidence level. It is worth to mention that these rates are the velocity of the whole Nubian plate plus the local deformation of the study area. The horizontal velocity of the Nubian plate is ranging between 25 and 28 mm/yr., which means that most of the achieved velocities rates are due to the movement of the Nubian plate. Therefore, to estimate the local deformation of the study area we have removed the movement of the Nubian plate.

Since our study area is relatively small, therefore we considered here that the average velocity of all sites is equal to the velocity of Nubia. Thus, a simple way to remove the velocity of Nubia from our estimates is to subtract the velocity of each site from the average velocity of the whole sites. This method is a simple approximation for the residual velocity estimation and the best way is to use the Euler poles of Nubia to compute the velocities in Nubia fixed frame. Table 1 presents

the location of the GPS site in the study area, the ITRF-08 velocities, the velocities in Nubia-fixed frame (velocities after removing the movement of the Nubian plate) and the scaled error (error estimated by scaling the co-variance matrix). As shown in Table 1 and Fig. 10, the horizontal velocity field for the study area in Nubia-fixed frame, the achieved velocities are in mm level. Most of Permanent sites show insignificant velocities with 95% of the confidence level. Except SHLA which moves toward the Northwest direction of 4 mm/yr. Sites West of Lake Nasser also do not show any significant horizontal velocity with respect to stable Nubia.

On the other hand, sites at Abu-Dabbab area showed a significant velocity with respect to Nubia. All Abu-Dabbab sites show inhomogeneous movement with different directions (rotational movement), and seem to be caused by the local seismic activity which characterized this area. The velocity rates of Abu-Dabbab sites is ranging from 1 to 4 mm/yr which is close to rates estimated by (Mohamed et al, 2013).

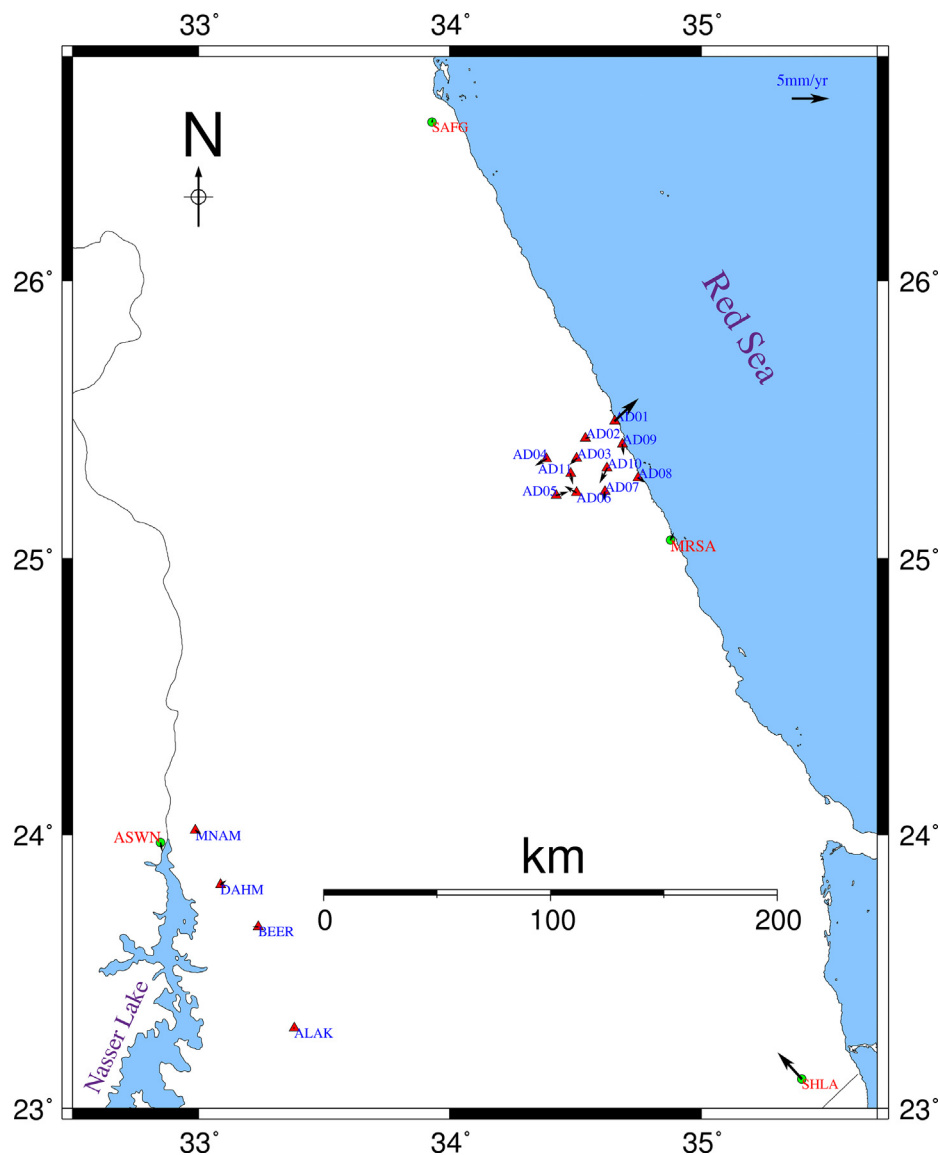


Fig. 10. Horizontal velocities for sites in the Southwestern part of Egypt in Nubia-fixed frame.

4. Discussion and conclusion

The main seismic cluster in this study area is Abu-Dabbab cluster, since the activities West of Lake Nasser are out the scope of this study. Two strong earthquakes of magnitude 6.1 M_b and 5.1 M_b were occurred on 12 November 1955, and 2 July 1984 respectively. Recent recording of the seismicity of Egypt showed a high rate of seismic activity within very small region at Abu-Dabbab area. The majority of earthquakes at Abu-Dabbab are micro-earthquakes, more than 90% have magnitudes less than 3.5 M_L and tend to align Northeast–Southwest perpendicular to Red Sea margin, as shown in Fig. 11. Many researchers interpret the tight seismicity cluster at Abu-Dabbab area as it due to intrusion of an igneous rocks. The heat flow observations at Abu-Dabbab area support this hypothesis (Morgan and Swanberg, 1978; Boulos et al., 1987, Mahmoud, 2003). On the other hand, other researchers do not believe that the seismic cluster at Abu-Dabbab is of magmatic nature, since there is no any localized magnetic or gravity anomalies recorded in Abu Dabbab area (Meshref, 1990).

In this study we have used eight years (2007–2014) of campaign

GPS data with four permanent stations (ASWN, SAFG, MRSA, and SHLA) to estimate the recent crustal movements in the Southeastern corner of Egypt. The absolute horizontal velocity field for the processed stations in ITRF08 with 95% confidence level showed a significant velocities for all sites of about 28 mm/yr toward the Northeast direction, which is quiet similar to the published rate by (Saleh and Becker 2014). In Nubia-fixed, most of GPS sites in the study area do not show any significant velocity with 95% of the confidence level, except the sites located at Abu-Dabbab area. The movements at Abu-Dabbab is $1-4 \pm \sim 2-3$ mm/yr. The high error values may be due to the presence of some outliers. Such a result is in good agreement with the recorded seismicity in the study area, As the only active region in the South-eastern corner of Egypt is Abu-Dabbab area.

We think that the spatial distribution of the GPS sites in the Southeastern part of Egypt is not optimum. Therefore, well distribution of the GPS stations will lead to better ground motion estimates for this region. Although the non-uniform distribution of the GPS sites in the Study area, our results are in good agreement with both tectonics and seismicity within the area. Other integrated geophysical and geodetic

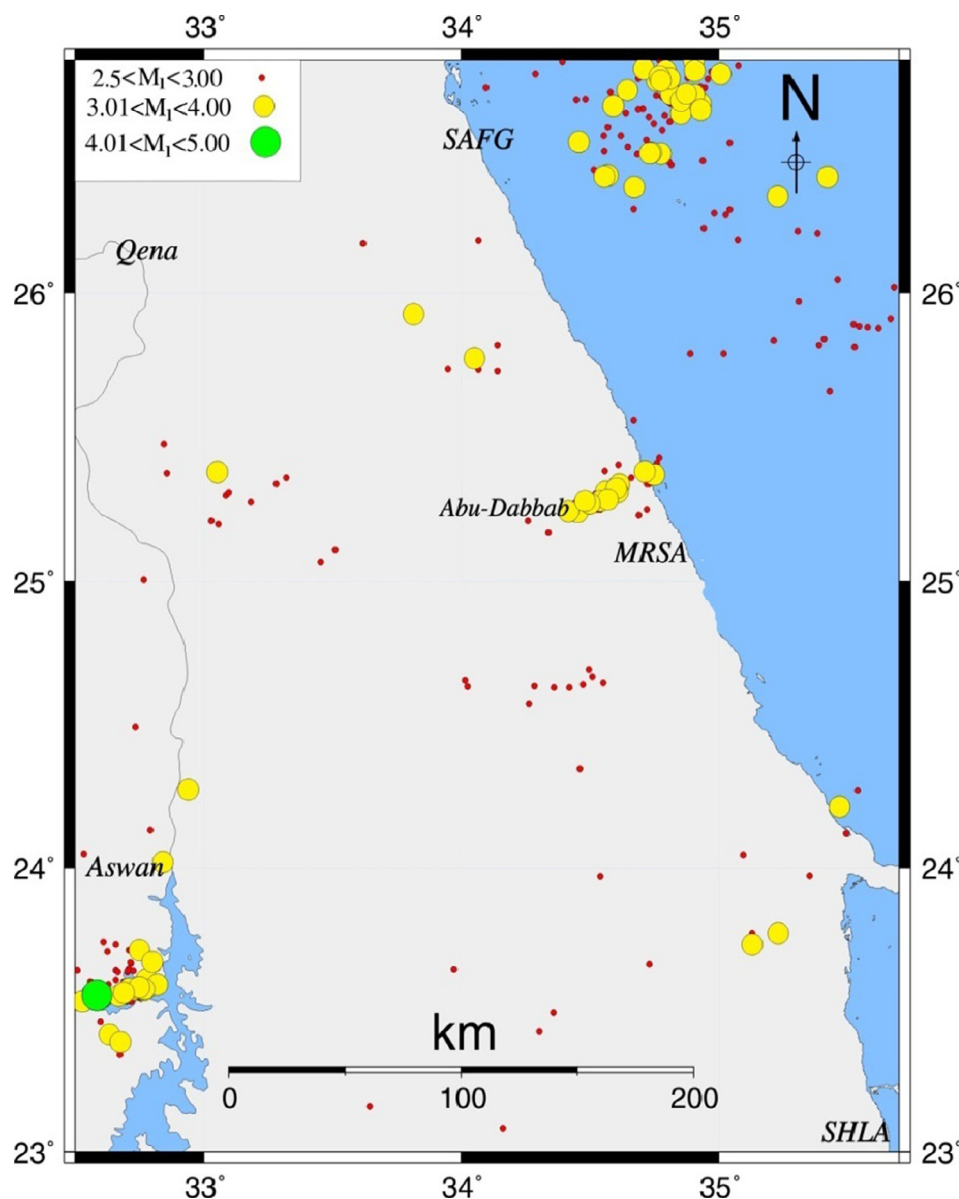


Fig. 11. Seismicity of the Southwestern part of Egypt between 2007 and 2014 (ENSN).

studies are needed to better understand the geodynamical behavior of the whole area and special interest should be given to Abu-Dabbab region. Our next job is to collect a new GPS dataset with a better spatial distribution in addition to apply the Interferometric Synthetic Aperture Radar (InSAR) for this area.

Acknowledgments

We thank the staff member of the Crustal Movement Laboratory, Geodynamic Department, NRIAG for providing GPS data. We are grateful to the supporters of the global IGS network and SOPAC. Most of Figures presented in this study are generated using Global Mapping Tool (GMT) software (Wessel and Smith, 1995).

References

- Abdeen, M.M., Abdelghaffar, A.A., 2011. Syn- and post-accretionary structures in the Neoproterozoic central Allaqi-Heiani suture zone, southeastern Egypt. *Precambrian Res.* 185, 95–108.
- Altamimi, Z., Collilieux, X., Métivier, L., 2011. ITRF2008: an improved solution of the international terrestrial reference frame. *J. Geodesy* 85 (8), 457–473.
- Badawy, A., El-Hady, S., Abdel-Fattah, A.K., 2008. Microearthquakes and neotectonics of Abu-Dabbab, eastern desert of Egypt. *Seismol. Res. Lett.* 79 (1), 55–67.
- Boulos, F.K., Morgan, P., Topozada, T.R., 1987. Microearthquake studies in Egypt carried out by the Geological Survey of Egypt. *J. Geodyn.* 7 (3), 227–249.
- Dach, R., Hugentobler, U., Fridez, P., Meindl, M. E. (2007). Bernese GPS Software Version 5.0 User Manual. Astronomical Institute, University of Bern.
- Egyptian Geological Survey and Mining Authority, EGSM (1981). *Geologic Map of Egypt*, 1:2,000,000.
- El Khrepy, S., Koulakov, I., Al-Arifi, N., 2015. Crustal structure in the area of the cannon earthquakes of Abu Dabbab (Northern Red Sea, Egypt), from Seismic Tomography Inversion. *Bull. Seismol. Soc. Am.* 105 (4), 13. <http://dx.doi.org/10.1785/0120140333>, (pp).
- Gass, I.G., 1982. Upper Proterozoic (Pan-African) Calc Alkaline Magmatism in Northeastern Africa and Arabia. In: Thorp, R.S. (Ed.), *Andesites*. Wiley, New York, pp. 91–609.
- Hussein, H.M., Moustafa, S.S.R., Elawadi, E., Al-Arifi, N.S., Hurukawa, N., 2011. Seismological aspects of the Abou Dabbab region, Eastern Desert, Egypt. *Seismol. Res. Lett.* 82 (1), 81–88.
- Hussein, H.M., Abou Elenean, K.M., Marzouk, I.A., Korrat, I.M., Abu El-Nader, I.F., Ghazala, H., ElGaby, M.N., 2013. Present-day tectonic stress regime in Egypt and surrounding area based on inversion of earthquake focal mechanisms (ISSN 1464-343X). *J. African Earth Sci.* 81, 1–15.
- Kröner, A., Todt, W., Hussein, I.M., Mansour, M., Rashwan, A.A., 1992. Dating of late Proterozoic ophiolites in Egypt and the Sudan using the single grain zircon evaporation technique. *Precambrian Res.* 59 (1–2), 15–32.
- Mahmoud, S.M., 2003. Seismicity and GPS-derived crustal deformation in Egypt. *J. Geodyn.* 35 (3), 333–352.
- Martinez, F., Cochran, J.R., 1988. Structure and tectonics of the northern Red Sea:

- catching a continental margin between rifting and drifting. *Tectonophysics* 150, 1–32.
- Meshref, W.M. (1990). Tectonic framework. In: Said, R., (Ed.), *The Geology of Egypt*, A. A. Balkema, Rotterdam, The Netherlands, 113–155 (Chapter 8).
- Mohamed, A.S., Hosny, A., Abou-Aly, N., Saleh, M., Rayan, A., 2013. Preliminary crustal deformation model deduced from GPS and earthquakes' data at Abu-Dabbab area, Eastern Desert, Egypt. *NRIAG J. Astronomy Geophys.* 2, 67–76.
- Morgan, P., Swanberg, C.A. (1978). Heat flow and the geothermal potential of Egypt, *Pure Appl. Geophys.* 117, Nos. 1/2, 213–226.
- Neumayr, P., Hoinkes, G., Puhl, J., Mogessie, A., Khudeir, A.A., 1998. The Meatiq dome (Eastern Desert, Egypt) a Precambrian metamorphic core complex: petrological and geological evidence. *J. Metamorphic Geol.* 16, 259–279.
- Saleh, M., Becker, M. 2014. A new velocity field from the analysis of the Egyptian Permanent GPS Network (EPGN). *Arab. J. Geosci.* <http://dx.doi.org/10.1007/s12517-013-1132-x>.
- Telesca, L., Fat-Elbary, R., Stabile, T.A., Haggag, M., Elgabry, M., 2017. Dynamical characterization of the 1982–2015 seismicity of Aswan region (Egypt). *Tectonophysics* 712713, 132–144 (ISSN 0040-1951).
- Wessel, R., Smith, W.H.F., 1995. New version of the generic mapping tools released. *Eos Trans. AGU* 76, 329.